Parallel Direct Numerical Simulation of Three-Dimensional Two-Phase Flows

Seungwon Shin [1], Jalel Chergui [2], Damir Juric[2], Asma Farhaoui [2], Lyes Kahouadji[2], Laurette S. Tuckerman[3], Nicolas Périnet[4]

[1]*Department of Mechanical and System Design Engineering, Hongik University, Seoul, 121-791 Korea*

[2]*LIMSI (UPR 3251 CNRS Univ. Paris Sud Paris XI) BP133, Rue J. von Neumann, 91403 Orsay, France*

[3]*PMMH (UMR 7636 CNRS-ESPCI-UPMC Paris 6-UPD Paris 7), 10 rue Vauquelin, 75005 Paris, France*

[4]*Departamento de física, FCFM, Universidad de Chile, Blanco Encalada 2008, 8370449 Santiago, Chile*

Keywords: Two-phase flow, direct numerical simulation, parallel high performance computing, front tracking, Faraday waves

Abstract

We present simulation results for several two-phase flow problems using a high performance, parallel code for the simulation of such incompressible flows in three dimensions. The code which we call BLUE is based on a high fidelity hybrid Front-Tracking/Level-Set algorithm for Lagrangian tracking of arbitrarily deformable phase interfaces including breakup and coalescence and a precise treatment of surface tension forces, interface advection and mass conservation. BLUE couples an implicit, incompressible Navier-Stokes solver with multigrid pressure solution to the Lagrangian tracking method for implementation on large-scale parallel computing architectures. The modular program structure allows for the application of the code to a wide variety of physical scenarios: free surface instabilities, flow of bubbles or drops with coalescence and breakup, droplet impact or flow around immersed solid objects for microchannel flows for example. We present simulations and evaluate the parallel numerical performance of BLUE for several physical phenomena of large spatio-temporal extent where high performance is indispensable: the canonical phenomenon of a water droplet splash onto a film of water, the merging of two bubbles and the Faraday instability in the highly nonlinear regime.

Introduction

Free-surfaces, films and general fluid-fluid interfaces are found in an extraordinary variety of situations and scales such as those in the study of free-surface waves, jets, bubbles and drops. The engineering applications of these structures alone range from microfluidics at the small scale (drop formation for micro-encapsulation) to marine engineering at larger scales (ocean waves, hull drag reduction by bubble injection) and bubbly flows in chemical engineering processes at scales in between. More complex coupled phenomena such as phase change in nucleate boiling have an impact on nearly all energy generation processes in which water must be turned to steam. The study of droplet formation and interaction in sprays has direct application to fuel injection and combustion and is usually coupled to species transport for the evolution of flame fronts. These are just a few examples to which free-surface codes have been applied by various research groups. Among the variety of interface methods developed in these applications (Volume of Fluid, Level Set, Phase field, Front-Tracking), the techniques our group are developing and working with are based on hybrid techniques, specifically a hybrid Front-Tracking/Level Set method which is considered to be more accurate, although more complex, than others.

Somewhat surprisingly, the proliferation of research and methods on interfaces developed by the computational fluid dynamics community and applied to engineering problems has not been as widely communicated in the fluid physics community for the study of free-surface instabilities, for example. Thus there is great potential that a capability such as the one described below could contribute to the elucidation of basic hydrodynamic experiments and their relation to larger questions in pattern formation, localized structures and dynamical systems. Indeed, our group was the first to fully simulate in three-dimensions the square and hexagonal patterns in the classic Faraday instability using the Front-Tracking method (Périnet et al 2009, 2012). Agreement with experiments was found to be quite good.

The area of numerical methods for free-surface and fluid interfaces has grown vastly in the last two decades. The presence of an interface and the ensuing non-linearities pose great difficulties for this branch of computational fluid dynamics due in part to the necessity to accurately compute surface tension forces and the need to provide a high fidelity treatment of these continuously evolving, deformable structures possibly including topology changes.

In this article we present results of simulations using a newly developed code for the simulation of two-phase incompressible flows. The high performance, parallel code, called BLUE was developed by three of the authors (S. Shin, J. Chergui and D. Juric). It uses our latest high-fidelity algorithms for Lagrangian tracking of arbitrarily deformable phase interfaces including breakup and coalescence and a precise treatment of surface tension forces, interface advection and mass conservation (Shin et al 2002, 2007, IJNMF 2009, 2011). BLUE is to our knowledge the first

implementation of such a hybrid Front-Tracking method on massively parallel architectures (up to tens of thousands of cores). The modular program structure allows for the application of the code to a wide variety of two-phase flow simulations: free-surface instabilities, flow of bubbles or drops with coalescence and breakup, thermal and species transport with phase change, droplet impact or flow around immersed solid objects for microchannel flows (see Fischer et al 2010, Shin et al JMST 2009, IJMF 2005 for examples). The code runs in single phase mode as well, for the simulation of simple incompressible flows. Additional physics modules for turbulence for example, could be developed and added as needed in the future.

Full details of the code structure and description of the parallel implementation of Lagrangian tracking and its coupling to the flow solver are beyond the scope of this article and will be presented in Shin, Chergui & Juric (2013). Here we present evaluations of the parallel numerical performance of BLUE as well as simulation results on the Faraday instability and the canonical cases of a water droplet splash into a pool of water and the merger of two bubbles. Our objective is the simulation of flows of very large spatio-temporal extent where high resolution and high performance is indispensable.

Numerical Scheme

In this work we limit our attention to two-phase isothermal flows. The governing equations for transport of an incompressible two-phase flow can be expressed by a single field formulation:

$$\nabla \cdot \mathbf{u} = 0 \tag{1}$$

$$\rho\left(\frac{\partial \mathbf{u}}{\partial t} + \mathbf{u}\cdot\nabla\mathbf{u}\right) = -\nabla P + \rho\mathbf{g} + \nabla\cdot\mu(\nabla\mathbf{u} + \nabla\mathbf{u}^{\mathrm{T}}) + \mathbf{F} \tag{2}$$

where **u** is the velocity, *P*, the pressure, **g**, the gravitational acceleration, and **F**, the local surface tension force at the interface. **F** is given by the hybrid formulation (Shin et al JCP 2005)

$$\mathbf{F} = \sigma\kappa_H \nabla I \tag{3}$$

where σ is the surface tension coefficient assumed to be constant. The indicator function, *I*, is essentially a numerical Heaviside function, ideally zero in one phase and one in the other phase. Numerically, *I* is resolved with a sharp but smooth transition across 3 to 4 grid cells and is generated using a vector distance function computed directly from the tracked interface (Shin & Juric IJNMF 2009). κ_H is twice the mean interface curvature field calculated on the Eulerian grid:

$$\kappa_H = \frac{\mathbf{F}_\mathrm{L}\cdot\mathbf{G}}{\mathbf{G}\cdot\mathbf{G}} \tag{4}$$

with

$$\mathbf{F_L} = \int_{\Gamma(t)} \kappa_f \mathbf{n}_f \delta_f(\mathbf{x}-\mathbf{x}_f)\mathrm{d}s \tag{5}$$

$$\mathbf{G} = \int_{\Gamma(t)} \mathbf{n}_f \delta_f\left(\mathbf{x}-\mathbf{x}_f\right)\mathrm{d}s \tag{6}$$

Here $\mathbf{x}_f$ is a parameterization of the time-dependent interface, $\Gamma(t)$, and $\delta(\mathbf{x}-\mathbf{x}_f)$ is a Dirac distribution that is non-zero only where $\mathbf{x}=\mathbf{x}_f$. $\mathbf{n}_f$ is the unit normal vector to the interface and *ds* is the length of an interface element. κ_f is twice the mean interface curvature obtained on the Lagrangian interface. The geometric information, unit normal, $\mathbf{n}_f$, and interface element length, *ds*, in **G** are computed directly from the Lagrangian interface and then distributed onto an Eulerian grid using the discrete delta function. A detailed description of the procedure for calculating the force and constructing the function field **G** and indicator function *I* can be found in Shin & Juric (IJNMF 2009).

The Lagrangian interface is advected by integrating

$$\frac{\mathrm{d}\mathbf{x}_f}{\mathrm{d}t} = \mathbf{V} \tag{7}$$

with a second order Runge-Kutta method where the interface velocity, **V**, is interpolated from the Eulerian velocity. Material properties such as density or viscosity are defined in the entire domain with the aid of the indicator function for the density for example :

$$\rho(\mathbf{x},t) = \rho_1 + (\rho_2 - \rho_1)I(\mathbf{x},t) \tag{8}$$

where the subscripts 1 and 2 stand for the respective phases.

The fluid variables **u** and *P* are calculated by means of a projection method (Chorin 1968, Goda 1979). A second-order Gear scheme is used for time integration. Either explicit or implicit time integration of the viscous terms may be chosen depending on the problem. For the spatial discretization we use the well-known staggered mesh, MAC method (Harlow & Welch 1965) with 2nd order ENO advection (Shu & Osher 1989, Sussman et al 1998). The pressure and distance function are located at cell centers while the *x*, *y* and *z* components of velocity are located at the faces. All spatial derivatives are approximated by standard second-order centered differences.

The code BLUE essentially consists of two modules:

- A module dedicated to the solution of the three-dimensional incompressible Navier-Stokes equations.
- A module for the treatment of the free surface using a parallel Lagrangian Tracking method. This module is only active if the flow is a two-phase flow.

BLUE is written in Fortran 2003 which allows the definition of a set of dynamically allocated derived [data] types and generic procedures associated with the matrix of procedures, grids, scalar and vector fields, operators as well as the various solvers used in the Navier-Stokes and Lagrangian Tracking modules.

The parallelization of the code is based on algebraic domain decomposition, where the velocity field is solved by a parallel GMRES method for the implicit viscous terms and the pressure by a parallel multigrid method (motivated by the algorithm of Kwak & Lee, 2004). Communication is handled by MPI message-passing procedures. The treatment of the fluid interfaces uses a hybrid Front-Tracking/Level-Set

technique which defines the interface both by a discontinuous density field as well as by a local triangular Lagrangian mesh. This structure allows the interface to undergo large deformations including the rupture and/or coalescence of fluid interfaces as occurs in the merging of bubbles or rupture of splashing drops. The code also contains a module for the definition of immersed solid objects and their interaction with the flow for both single and two-phase flows. In the two-phase case a contact line model for the interaction of the fluid interface with the solid object is included.

Results and Discussion

There are two ways to evaluate the performance of parallel codes. The "heavy scaling" evaluation is based on program execution timings with varying number of cores (processors) while keeping the global mesh resolution fixed. The "weak scaling" evaluation is based on program execution timings with varying number of cores while keeping the local (subdomain) resolution fixed. In BLUE, we are more concerned with the latter for two main reasons: (1) On the BlueGene machines each core has a small memory of 512MB and (2) we are more concerned with using the maximum number of cores (subdomains) available for a fixed local mesh resolution per core in order to attain the finest global mesh resolution possible.

BLUE has been successfully run on up to 8192 cores on the BlueGene/P and /Q machines at IDRIS in Orsay, France and on 16384 cores on the BlueGene/Q at the Julich Supercomputing Center (JSC), Germany with excellent linear scalability performance as shown in figures 1 and 2 for the drop splash calculation of figure 3.

Fixing 32×32×32 as the resolution per core and using up to 8192=16×16×32 cores gives a global resolution of 512×512×1024. The speedup and efficiency of BLUE for weak scaling is defined as:

$$S = \frac{Nc}{Nc_{ref}} \times E \qquad (9)$$

where Nc is the number of cores, Nc_{ref} is the reference number of cores (here 128) and E represents efficiency defined as :

$$E = \frac{Tc_{ref}}{Tc} \qquad (10)$$

where Tc_{ref} is the elapsed time measured for Nc_{ref} = 128 cores. Tc is the elapsed time measured for Nc = 512, 1024, 2048, 4096, or 8192 cores, respectively. We show the speedup with number of cores in figure 1. As expected, the scalability of the code is sufficient to overcome communication overhead as the number of cores increases. Up to 8192 cores, speedup is quite linear. The efficiency shown in figure 2 demonstrates that the average core utilization is about 68% and is maintained constant up to 8192 cores. Due to the machine memory architecture limitations we cannot perform a heavy scaling study; nevertheless we can deduce from the weak scaling study that choosing a global mesh resolution of 512×512×1024 on 8192 cores, the code runs 42 times faster than it would have on 128 cores.

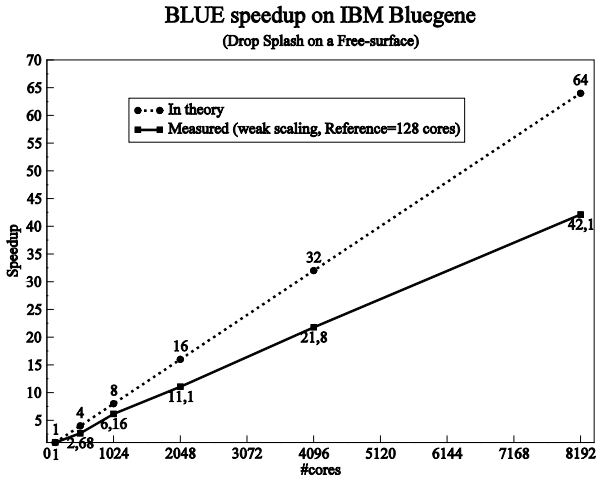

Figure 1 : Performance increase with number of cores.

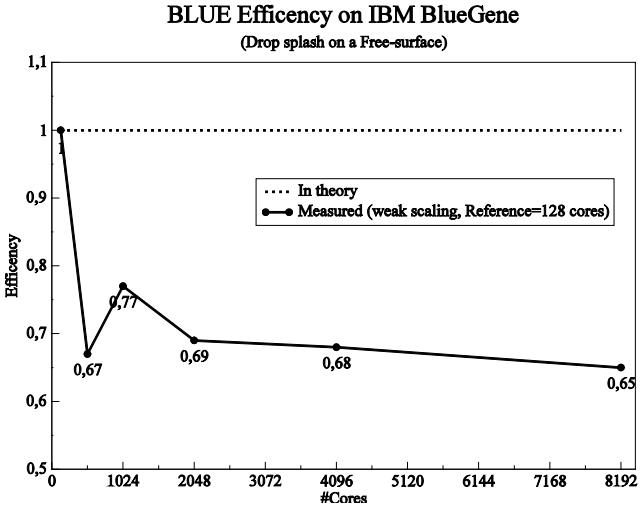

Figure 2 : Efficiency vs. number of cores.

We now present the results of highly resolved 3D calculations for three example problems: the splash of a drop on a liquid free surface, the merging of two bubbles and free-surface evolution in the Faraday instability.

In the first example a water drop of radius 4.53 mm splashes onto a 1 mm thin film of water at an initial vertical speed of 2.193 m/s. The calculation domain is a closed square box 3.6 cm on a side resolved by a 512^3 Cartesian mesh. The domain is decomposed into 4096 subdomains each at a resolution of 16^3 for parallel computation on 4096 cores. A sequence of six snapshots is shown in figure 3 at times 2.3ms, 3.45ms, 6.01ms, 7.84ms, 8.65ms and 17.7ms. The nearly spherical drop impacts the film at high velocity to create a crater whose sides rise while expanding outwards from the impact site. The crater walls begin to break up into droplets. In figure 4 velocity vectors on a vertical slice through the midplane illustrate the evolution of the velocity field and in particular a vortical motion of in-rushing air around the lip of the crater as the wall of water rises and expands. This inward curling motion is due to the expansion and rise of the ring of water in conjunction with the constraints of the side walls of the closed box (no slip and no penetration conditions on all 6 faces).

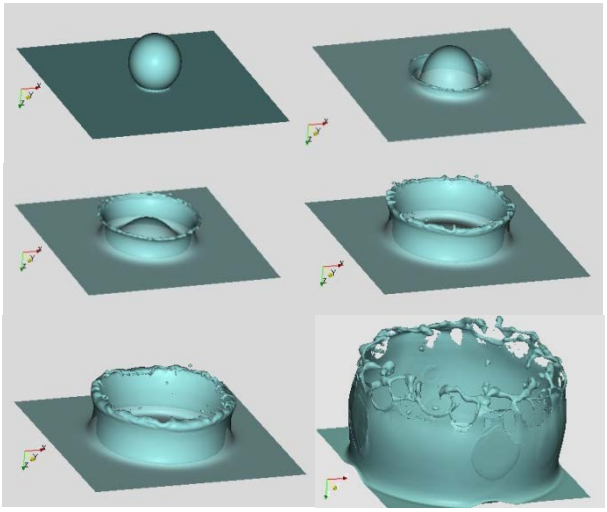

Figure 3 : Sequence (read left to right and top to bottom) of 6 snapshots of the simulation of a water drop splash onto a free-surface of water. Parallel 3D simulation on 4096 cores of the BlueGene/Q supercomputer at JSC, Germany.

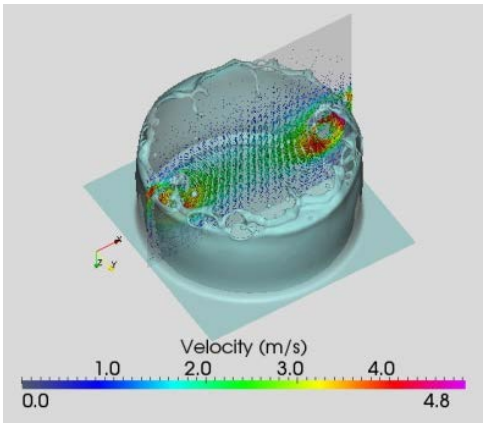

Figure 4 : Velocity vectors on a vertical mid-plane slice for a snapshot of the simulation in figure 3 at 14.7ms.

The second example shown in figure 5 presents the problem of two air bubbles rising through water and their process of merging. The two bubbles (lower bubble of radius 1cm and upper bubble of radius 2 cm) are initially placed slightly off the vertical center axis resulting in non-symmetric merging. The calculation domain is a closed rectangular box of dimensions (L_x, L_y, L_z) = (10cm, 10cm, 20cm) resolved by a 256×256×512 Cartesian mesh. The domain is decomposed into 2×2×8=32 subdomains (whose traces can be seen in figure 5) each at a resolution of 128×128×64. A sequence of eight snapshots is shown at times 2.95ms, 18.8ms, 32ms, 39.7ms, 50.8ms, 65.7ms, 82.9ms and 118ms. For these two relatively large bubbles, the merging process is extremely rapid and induces large deformations in the joined bubble surfaces. In the close-up of figure 6, a jet of air resulting from the high local surface tension forces during merging can be seen pushing through the top bubble, deforming it greatly.

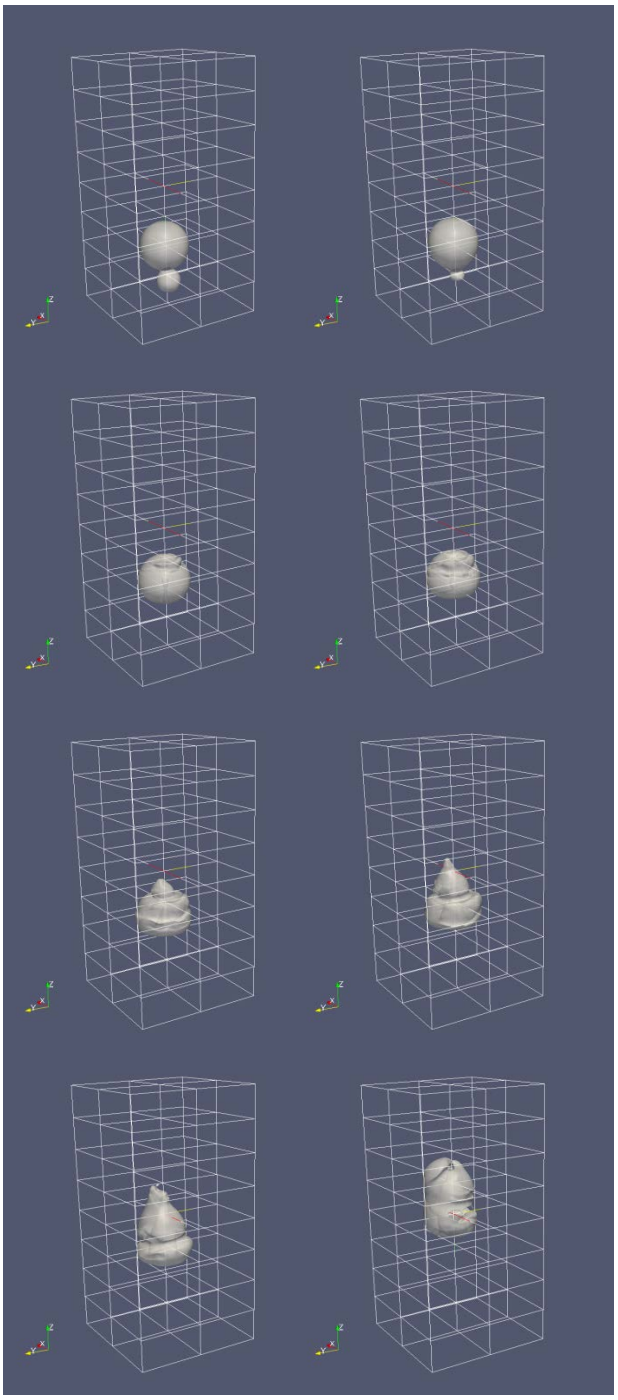

Figure 5 : Sequence (read left to right and top to bottom) of 8 snapshots of the simulation of the off axis rise of two air bubbles through water and subsequent merging.

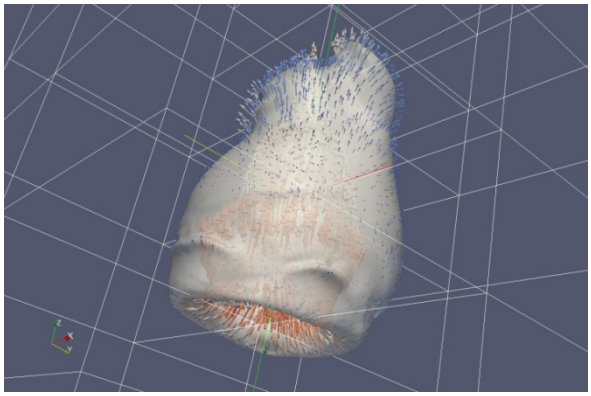

Figure 6 : Closeup of the merged bubbles from figure 5 at t=102ms with velocity vectors plotted on the interface.

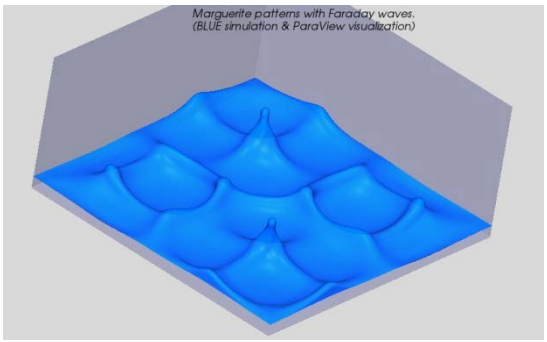

Figure 7 : High-amplitude Faraday waves appear when a 7mm deep oil film is vibrated at amplitude 1g and frequency 10Hz in a 17cm×17cm×8cm container resolved by a 512×512×256 mesh. Parallel 3D two-phase simulation using the code BLUE on 2048 cores of the BlueGene/P supercomputer at IDRIS, France.

The next examples are those of the parametrically driven free-surface instability discovered by Michael Faraday (1831) who conducted a simple experiment which consisted of shaking vertically a container containing two immiscible fluids (the lighter of which can be air) thereby inducing oscillations of the fluids and the interface between them. Beyond a certain threshold, the interface can form many kinds of standing-wave patterns such as stripes, squares, hexagons and more exotic motifs whose study is of current interest. In figure 7 we present a simulation motivated by the experiments of J. Rajchenbach et al. (2013) (see video, Rajchenbach 2012) which show the formation of an intriguing five-fold symmetric, marguerite flower pattern. For the Faraday simulations the acceleration **g** in equation 2 is taken to be $\mathbf{g}=(a\cos(\omega t) - g)\boldsymbol{e}_z$ thus effectively transforming into a reference frame oscillating with a periodic acceleration of amplitude, a, and frequency, ω.

In the simulation in figure 7 (Farhaoui, 2012) alternating square and octagonal high amplitude Faraday waves appear when a 7mm deep oil film (density 928.8 kg/m^3, absolute viscosity 0.092 kg/m/s, surface tension 0.02 kg/s^2) is vibrated at amplitude 1g and frequency 10Hz in a 17cm × 17cm × 8cm container resolved by a 512×512×256 mesh.

The appearance of pentagonal forms in figures 8 and 9 matches another set of experimental observations (Pucci & Couder, 2011) for the vibration of a 1.45cm deep layer of oil (density 965 kg/m^3, absolute viscosity 0.02 kg/m/s, surface tension 0.02 kg/s^2) at 1.5g and 30Hz. The experiment was simulated in a 10cm x 10cm x 5cm domain resolved by a 256×256×128 mesh on 4×4×2=32 subdomains (cores) each at a resolution of 64^3. Figure 8 shows the interface colored by its vertical velocity as well as velocity vectors on a vertical slice of the domain. The top view in figure 9 shows more clearly the pentagonal forms on the interface.

The Floquet threshold for these values of the fluid parameters was calculated using the method of Kumar & Tuckerman (1994) and compared to that obtained numerically and experimentally. Table 1 shows the comparisons for the normalized critical accelerations, a_c/g,

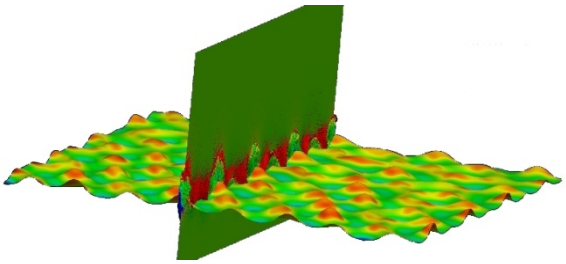

Figure 8 : Simulation of the Pucci (2011) experiment for the vibration of a 1.45cm deep layer of oil at 1.5g and 30Hz. The experiment was simulated in a 10cm × 10cm × 5cm domain resolved by a 256×256×128 mesh on 4×4×2=32 subdomains (cores) each at a resolution of 64^3.

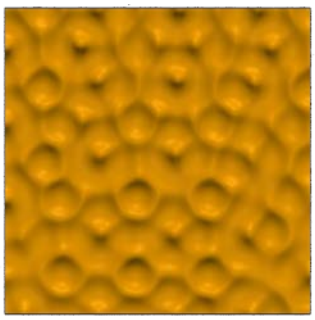

Figure 9 : Top view illustrating non-periodic pentagonal motifs for the interface in figure 8.

obtained at three different vibration frequencies, ω. The numerical results were calculated in a horizontally periodic domain of dimensions, $(L_x, L_y, L_z) = (\lambda_c, \lambda_c/2, 2\lambda_c)$ with λ_c being the critical wavelength calculated by Floquet theory of the most unstable mode. The agreement among the three threshold acceleration values is quite good.

Table 1: Comparison of Floquet, numerical and experimental instability thresholds for the simulation shown in figures 8 and 9 with varying vibration frequency

$\omega/2\pi$ Hz	λ_c mm	Floquet a_c/g	num. a_c/g	exp. a_c/g	% error Floquet/num.
30	11.3	0.733	0.723	0.74	1.4
60	5.9	2.65	2.61	2.52	1.5
90	4.3	5.32	5.30	4.98	0.38

Experiments designed to study the dynamics and interactions of solitons in a hydrodynamic channel are described in Clerc et al. (2011) and Gordillo et al. (2011) and simulated using BLUE on 4×2×4=32 cores of an IBM iDataplex cluster at the Center for Mathematical Modeling, Universidad de Chile. Figure 10 shows back (top figure) and front (bottom figure) views of the 19 cm long × 2.54 cm wide × 6 cm high channel resolved by a 124×64×128 mesh. The channel is filled to a depth of 2cm with a mixture of water and Kodak Photo flo® 200, added for improved wall wetting (density 1100 kg/m^3, absolute viscosity 0.001138 kg/m/s, surface tension 0.035 kg/s^2) then vibrated at amplitude 0.1g and frequency 10.6Hz. Velocity vectors (not to scale, color represents the velocity magnitude, red is maximum and blue is zero) show the vortical structures formed around a transversely sloshing soliton.

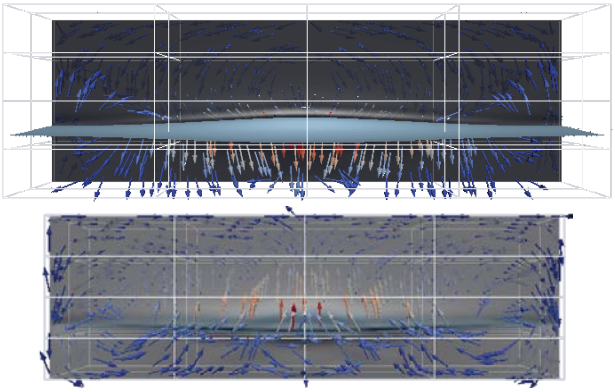

Figure 10 : Views of the soliton simulation using BLUE on 4×2×4=32 cores of an IBM iDataplex cluster at the Center for Mathematical Modeling, Universidad de Chile for a 19 cm long × 2.54 cm wide × 6 cm high channel resolved by a 124×64×128 global mesh. Velocity vectors (not to scale, color represents the velocity magnitude, red is maximum and blue is zero) show the vortical structures formed around a transversely sloshing soliton due to vibration at amplitude 0.1g and frequency 10.6 Hz. Gray-leveled slices represent the transverse (*y*) component of the velocities (brighter shade represents larger *y*-velocity component). Top: vectors and slice are plotted 2mm from the back wall. Bottom: vectors and slice are plotted 2mm from the front wall.

Conclusions

We have demonstrated the capabilities of BLUE, a new high performance parallel numerical code for the simulation of two-phase incompressible flows. The code combines high-fidelity algorithms for Lagrangian tracking of deformable phase interfaces for a precise treatment of surface tension forces, interface advection and mass conservation. The parallel structure has made it possible to carry out calculations on highly refined grids of extremely deformed interfaces including rupture and coalescence as in the examples presented in this work of merging bubbles, splashing drops and the Faraday free-surface instability. BLUE is, to our knowledge the first implementation of Lagrangian tracking on massively parallel architectures and has been run on up to 8192 cores on the BlueGene/P machine at the CNRS IDRIS computing center in Orsay, France and on 16384 cores on the BlueGene/Q machine in Julich, Germany with excellent scalability performance.

Acknowledgements

This work was supported by GENCI Project i20132b6721 at IDRIS, France, by PRACE project PRA074 at JCS, Germany and by Basic Science Research Program through the National Research Foundation of Korea (NRF) funded by the Ministry of Education, Science and Technology (2012R1A1A2004478). All images have been post processed with ParaView.

References

Faraday, M. On a peculiar class of acoustical figures; and on certain forms assumed by groups of particles upon vibrating elastic surfaces. Phil. Trans. R. Soc. Lond. Vol. 121, 299–340 (1831).

Chorin J. Numerical solution of the Navier–Stokes equations. Mathematics of Computation, Vol. 22, 745–762 (1968).

Clerc, M.G., Coulibaly, S., Gordillo, L., Mujica, N. & Navarro, R. Coalescence cascade of dissipative solitons in parametrically driven systems, Phys. Rev. E, Vol. 84, 036205 (2011).

Goda, K. A multistep technique with implicit difference schemes for calculating two- or three-dimensional cavity flows, J. Comput. Phys., Vol. 30, 76 (1979).

Gordillo, L., Sauma, T., Zarate, Y., Espinoza, I., Clerc, M.G. & Mujica, N., Can non-propagating hydrodynamic solitons be forced to move? Eur. Phys. J. D, Vol. 62(1), 39-49 (2011).

Harlow, F.H. & Welch, J.E. Numerical calculation of time dependent viscous incompressible flow of fluid with free surface. Phys. Fluids, Vol. 8, 2182–2189 (1965).

Farhaoui, A. Simulation numérique des ondes de Faraday sous forme de motifs pentagonaux, Master's Thesis report, Univ. Paris XI, LIMSI Report N° 2012-17 (2012).

Fischer, M., Juric, D. & Poulikakos, D. Large convective heat transfer enhancement in microchannels with a train of co-flowing immiscible or colloidal droplets, J. Heat Transfer, Vol. 132, 112402-1-10 (2010).

Kumar, K. & Tuckerman, L.S. Parametric instability of the interface between two fluids. J. Fluid Mech. Vol. 279, 49-68 (1994).

Kwak, D.Y., Lee, J.S. Multigrid Algorithm for the Cell-Centred Finite Difference Method II: Discontinuous Coefficient Case. Wiley InterScience (www.interscience.com). DOI 10.1001/num.20001 (2004).

Périnet, N., Juric, D. & Tuckerman, L.S. Numerical simulation of Faraday waves, J. Fluid Mech. Vol. 635, 1-26 (2009).

Périnet, N., Juric, D. & Tuckerman, L.S. Alternating hexagonal and striped patterns in Faraday surface waves, Phys. Rev. Lett. Vol. 109, 164501 (2012).

Pucci, G. & Couder, Y. Laboratoire Matières et Systèmes Complexes (MSC), Université Paris 7 Diderot, private communication (2011).Tapez une équation ici.

Rajchenbach, J., Clamond, D. & Leroux, A. Observation of star-shaped surface gravity waves, Phys. Rev. Lett. preprint (2013).

Rajchenbach, J. private communication (2012). http://www.newscientist.com/blogs/nstv/2012/10/star-shaped-waves-wobbly-oil.html

Shin, S., Chergui, J. & Juric, D. BLUE: A platform for parallel direct numerical simulation of three-dimensional two-phase flows, in preparation (2013).

Shin, S., Yoon, I. & Juric, D. The Local Front Reconstruction Method for direct simulation of two-and three-dimensional multiphase flows, J. Comput. Phys. Vol. 230, 6605-6646 (2011).

Shin, S. & Juric, D. A hybrid interface method for three-dimensional multiphase flows based on front-tracking and level set techniques, Int. J. Num. Meth. Fluids, Vol. 60, 753-778 (2009).

Shin, S. & Juric, D. High order level contour reconstruction method, J. Mech. Sci. Technol., Vol. 21, 311-326 (2007).

Shin, S. & Juric, D. Modeling three-dimensional multiphase flow using a level contour reconstruction method for front tracking without connectivity, J. Comput. Phys., Vol. 180, 427-470 (2002).

Shin, S. & Juric, D. Simulation of droplet impact on a solid surface using the level contour reconstruction method, J. Mech. Sci. Technol., Vol. 23, 2434-2443 (2009).

Shin, S., Abdel-Khalik, S.I. & Juric, D. Direct Three-Dimensional Numerical Simulation of Nucleate Boiling using the Level Contour Reconstruction Method, Int. J. Multiphase Flow, Vol. 31, 1231-1242 (2005).

Shin, S., Abdel-Khalik, S.I., Daru V. & Juric, D. Accurate Representation of Surface Tension Using the Level Contour Reconstruction Method, J. Comput. Phys., Vol. 203, 493-516 (2005).

Shu, C.W. & Osher, S. Efficient implementation of essentially non-oscillatory shock capturing schemes II. J. Comput. Phys, Vol. 83, 32–78 (1989).

Sussman, M., Fatemi, E., Smereka, P. & Osher, S. An improved level set method for incompressible two-phase flows, Computers and Fluids, Vol. 27, 663–680 (1998).